Springer
Acta Mechanica Sinica
CrossMark click for updates
• RESEARCH PAPER •
Acta Mech. Sin., Vol. 41, 323513 (2025)
https://doi.org/10.1007/s10409-024-23513-x

Thermodynamics performance assessment of precooled cycle engines with ammonia as the fuel and coolant

Xin Zhang[1,2], Yang Lu[1,2*], and Xuejun Fan[1,2]

[1] *State Key Laboratory of High Temperature Gas Dynamics, Institute of Mechanics, Chinese Academy of Sciences, Beijing 100190, China;*
[2] *School of Engineering Science, University of Chinese Academy of Sciences, Beijing 100049, China*

Received January 10, 2024; accepted March 5, 2024; published online September 9, 2024

To meet the demand for air-breathing power for wide-range vehicles at Mach 0-10, two thermal cycles with ammonia as the fuel and coolant were analyzed, namely the precooled rocket-turbine cycle (PC-RT) and the precooled gas-turbine cycle. Firstly, the operating modes of the precooled cycle engines were divided into turbine mode, precooling mode, and ramjet mode. Secondly, a fluid-structure coupling heat transfer program was used to evaluate the cooling effects of different fuels on the incoming high-temperature air. The result shows that the equivalent heat sink of ammonia is higher than that of other fuels and can meet the cooling requirement of at least Mach 4 in the precooling mode. Thirdly, the performance of the PC-RT in the turbine and precooling modes was compared at Mach 2.5. The result shows that air precooling alleviates the restriction of the pumping pressure on the minimum required β and improves the specific thrust within a reasonable range of β. Fourthly, the performance of the precooled cycle engines was compared when using different fuels. The result shows that the specific thrust of ammonia is greater than that of other fuels, and the performance advantages of ammonia are the most obvious in the precooling mode due to its highest equivalent heat sink. To sum up, the precooled cycle engines with ammonia as the fuel and coolant presented in this study have the advantages of no carbon emissions, low cost, high specific thrust, and no clogging of the cooling channels by cracking products. They are suitable for applications such as the first-stage power of the two-stage vehicle, and high Mach numbers air-breathing flight.

Ammonia, PC-RT, PC-GT, Specific thrust, Specific impulse

Citation: X. Zhang, Y. Lu, and X. Fan, Thermodynamics performance assessment of precooled cycle engines with ammonia as the fuel and coolant, Acta Mech. Sin. 41, 323513 (2025), https://doi.org/10.1007/s10409-024-23513-x

1. Introduction

Ultra-fast, economical, and green traveling is pursued in the foreseeable future. In order to meet the demands of the wide-speed range and long-time working capability, concepts of variable cycle and combined engines were proposed [1,2]. Among them, the turbine-based combined cycle (TBCC), with its advantages of horizontal takeoff and landing, low oxidant carrying requirement, and high reliability, is one of the most promising power system solutions and has become the focus of research in recent years [3,4]. However, the scramjet engine cannot provide sufficient thrust below Mach 4, and the existing turbine engine cannot provide sufficient thrust above Mach 2.5 due to the constraint of the compressor exit temperature, resulting in a thrust gap problem [1,5]. To solve the problem, researchers have proposed a solution to increase the maximum operating Mach numbers of the turbine engine by cooling the incoming air with onboard coolant.

There are two main ways to achieve air precooling: mass injection precooling and heat exchanger precooling [6,7]. Mass injection precooling is carried out by mixing coolant into the incoming high-temperature air through an additional injection device in front of the compressor to keep the air temperature at the compressor exit within the upper tolerable limit. It causes a pressure loss of the intake airflow, and the injection of the general water-based cooling medium results in a reduction in the oxygen content of the air, so the

*Corresponding author. E-mail address: luyang@imech.ac.cn (Yang Lu)
Executive Editor: Jianqiang Chen

© The Chinese Society of Theoretical and Applied Mechanics and Springer-Verlag GmbH Germany, part of Springer Nature 2024

maximum flight Mach numbers achievable with this method are generally not high. For example, the mass injection pre-compressor cooling (MIPCC), based on the F100 engine of the United States, is designed with a maximum Mach number of 3.5 and a flight altitude of 25 km [8]. In Ref. [9], an ammonia MIPCC aeroengine was proposed and its performance was evaluated, providing a new idea for the application of ammonia in mass injection precooling. Heat exchanger precooling includes fuel-direct precooling and indirect precooling by introducing an intermediate medium. For example, the air-turbo ramjet with expander cycle (ATREX) directly uses liquid hydrogen as the coolant, with heat exchange components installed in the intake and near the combustor, and drives the turbine through coolant expansion [10-12]. The precooled turbojet engine (PCTJ) also directly uses liquid hydrogen as the coolant. After completing the heat exchange with air in the precooler, some of the fuel reacts with pressurized air in the main combustor to produce oxygen-rich gas to drive the turbine, and the remaining is added into the afterburner to further burn with the oxygen-rich gas expanded from the turbine [13,14]. The synergetic air breathing rocket engine (SABRE) uses an indirect precooling mode, which introduces a closed helium cycle between hydrogen and air, and uses cold helium to cool hot air while reducing hydrogen embrittlement [15,16].

Selecting suitable propellants is indispensable to realize the wide-range operation for air-breathing engines. The ideal propellants must have sufficient energy density and heat sink. Many studies have shown that hydrogen can meet these requirements, but the use of hydrogen is difficult and costly due to its low-temperature and low-density properties [17,18]. Some researchers have turned their attention to other fuels. Yu et al. [19] compared the performance of fuels such as hydrogen, methane, decane, and methanol in terms of specific thrust, specific impulse, and vehicle flight range. The result shows that although the specific impulse of a hydrogen-fueled engine is much larger than that of other fuels, the corresponding flight range is the smallest due to the low-density properties of hydrogen. Lu and Fan [20] proposed a fuel-rich precooled combined cycle engine using methane as the fuel and coolant, and preliminarily verified its feasibility to operate from low altitude and low speed up to Mach 7. In Ref. [21], alcohol fuel was introduced to the chemical precooled turbine engine cycle. The result shows that increasing the fuel cracking rate can reduce fuel consumption for air precooling and improve the specific impulse of the engine. In Ref. [22], ammonia was introduced to the chemical precooled turbine engine cycle. It is assumed that ammonia cracks well in the precooler at Mach 3-4 flight conditions, that cracking can occur at 300 K, and that the cracking rate of ammonia has reached more than 70% at 700 K. Also in Ref. [23], it is assumed that ammonia cracks at 300 K and that the increased chemical heat sink from cracking cools the incoming high-temperature air at 300-800 K effectively. On the other hand, in Ref. [24], the cracking rates of ammonia without catalysts were measured experimentally, showing that the initial cracking temperature of ammonia is about 873 K. There is a bias between the two. The reason is that in Refs. [22,23], the cracking rate of ammonia is derived from chemical equilibrium calculations of the cracking reaction. Different catalysts have been studied to lower the initial cracking temperature of ammonia. According to Refs. [25-27], the initial cracking temperature of ammonia is rarely below 650 K using most catalysts in practice. Thus, for Mach 3-4 flight conditions, ammonia cannot be supposed to have a high cracking rate in the precooler without special treatment. In Ref. [28], according to the ammonia cracking rate curve in Ref. [26], it is proposed that the cracking rate of ammonia in the precooler at Mach 5 flight condition is about 65% when the equivalence ratio is 1.0. The cracking rate is about 7% at Mach 4 flight condition, and ammonia cannot crack at Mach 3 flight condition when the equivalence ratio is 1.0. However, in Ref. [28], ammonia is merely considered to absorb heat from the precooler, which limits a further increase in the cracking rate. In fact, under all conditions, the combustor also needs to be cooled to keep the temperature within the upper tolerable limit. In this study, in addition to the precooler, the regenerative cooling heat exchanger is also placed on the combustor. Therefore, ammonia is heated in the precooler and the regenerative cooling heat exchanger to further increase the cracking rate and hydrogen content, which promotes combustion. On the system level, the incoming air and the combustor can be cooled by ammonia, which results in a performance improvement.

In this study, two thermal cycles are closely examined. According to the different working mediums used to drive the turbine to do work, they are named the precooled rocket-turbine cycle (PC-RT) and the precooled gas-turbine cycle (PC-GT) [29]. “Rocket” here means that just like the rocket engine, the source of the turbine-driven fluid for this cycle is the onboard fuel or oxidizer. The source of the turbine-driven fluid for the PC-GT is the high-temperature oxygen-rich gas. The application of ammonia as the fuel and coolant in the precooled cycle engines based on the PC-RT and PC-GT is studied by numerical simulation and theoretical analysis. The cracking rate of ammonia and the corresponding air temperature after cooling in the precooler were evaluated at different Mach numbers. The variation of the engine performance as the cracking rate increases is discussed using ammonia as the fuel and coolant. And the performance of ammonia is compared with that of conventional fuels such as hydrogen, methane, and kerosene. And the performance of the PC-RT and PC-GT is also compared. The study provides a useful reference and technical support for engine design when ammonia is used as the coolant and cracked ammonia is used as the fuel in the precooled cycle engines.

Taking the PC-RT as an example, the energy transfer process is shown in Fig. 1. Q_p is the heat absorbed by the fuel in the precooler corresponding to a unit mass of air. Q_r is the heat absorbed by the fuel from the combustor corresponding to a unit mass of air. After absorbing the heat from Q_p and Q_r, the liquid ammonia cracks into nitrogen and hydrogen, and the ammonia-nitrogen-hydrogen mixture expands and drives the turbine to compensate for the work consumed by the fuel pump (W_P) and the compressor (W_C).

2. Analysis of fuel characteristics

Reference [28] proposed to use the equivalent calorific value to measure the theoretical maximum amount of heat that can be provided per unit mass of incoming air by the fuel combustion when the equivalence ratio is 1.0.

$$Q = f_{st} \cdot h_{PR}, \tag{1}$$

where Q is the equivalent calorific value of the fuel, MJ/kg; f_{st} is the fuel-air mass flow ratio at the equivalence ratio of 1.0; h_{PR} is the net calorific value of the fuel, MJ/kg. For ammonia, kerosene, methane, and hydrogen, f_{st} is 0.165, 0.067, 0.058, and 0.029, respectively.

The comparison of the equivalent calorific value for several fuels has been shown in Ref. [28]. Hydrogen has the highest equivalent calorific value among the four fuels, followed by ammonia. Although ammonia has the lowest net calorific value, it ultimately has a higher equivalent calorific value than methane and kerosene because it has the highest fuel-air mass flow ratio at the equivalence ratio of 1.0. For ammonia, kerosene, methane, and hydrogen, the equivalent calorific value is 3.07, 2.97, 2.91, and 3.50 MJ/kg, respectively.

Reference [28] proposed to use the equivalent heat sink to measure the cooling capacity of fuel when the equivalence ratio is 1.0,

$$Q_f = f_{st} \cdot h_{fc}, \tag{2}$$

where Q_f is the equivalent heat sink of the fuel, kJ/kg; h_{fc} is the total heat sink (physical heat sink + chemical heat sink) absorbed by per unit mass of the fuel from storage conditions (stored in liquid state) to 1000 K, kJ/kg. In this study, it is assumed that the storage temperature of cryogenic fuels in the tank is their corresponding boiling point temperature at atmospheric pressure, and the storage temperature of kerosene is 293 K.

The comparison of the equivalent heat sink for several fuels has also been shown in Ref. [28]. Ammonia has the highest equivalent heat sink among the four fuels, followed by hydrogen. Because ammonia has the highest fuel-air mass flow ratio at the equivalence ratio of 1.0, and the cracking reaction further increases its equivalent heat sink. For ammonia, kerosene, methane, and hydrogen, the equivalent heat sink is 742.5, 219.8, 194.3, and 414.5 kJ/kg, respectively.

According to Refs. [24-26], ammonia cracks into hydrogen and nitrogen in the microchannel at high-temperature conditions. The standard enthalpy of ammonia cracking is 2717 kJ/kg. The chemical equation of ammonia cracking is $2NH_3 \rightarrow N_2 + 3H_2$.

As shown in Fig. 2, Ref. [26] used the computational fluid dynamics (CFD) method to calculate the ammonia cracking rate curve when using ruthenium as the catalyst in the microreactor with a size of area/volume = 31 cm^{-1} and compared it with the experimental values to verify the accuracy of the calculation method. Then, the cracking rate curve of ammonia in the microreactor without the catalyst was calculated with a size of area/volume = 38.15 cm^{-1} (equivalent to a channel inner diameter of 1.05 mm) under heating conditions. The cracking rate curve without the catalyst is chosen as the basis for the ammonia cracking rate calculation in this study.

Figure 3 shows the calculated results of the ammonia heat sink, where the total heat sink refers to the sum of the physical heat sink and chemical heat sink. The standard enthalpy of ammonia cracking is 2717 kJ/kg, which means that ammonia will absorb 2717 kJ/kg of heat when it completely cracks into nitrogen and hydrogen at 298.15 K. Taking the temperature of 1000 K as an example, as shown in Fig. 4, the calculation of the heat of reaction at 1000 K can be broken down as follows: imagine that the temperature of ammonia is first lowered from 1000 to 298.15 K, which gives off 1988 kJ/kg of heat (the negative sign represents exothermic), and then it completely cracks into nitrogen and hydrogen at 298.15 K, which absorbs

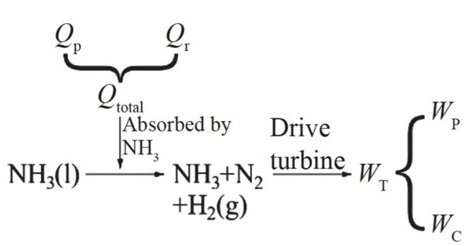

Figure 1 Schematic of energy transfer for the PC-RT.

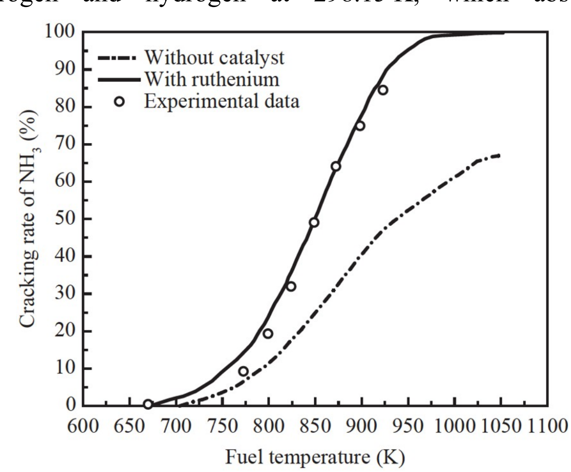

Figure 2 Cracking rate curve of ammonia in the microchannel [26].

2717 kJ/kg of heat, and then the nitrogen-hydrogen mixture is heated to 1000 K, which absorbs 2452 kJ/kg of heat. In summary, ammonia will absorb 3180 kJ/kg of heat when it completely cracks into nitrogen and hydrogen at 1000 K. According to the cracking rate curve of ammonia shown in Fig. 2, the cracking rate of ammonia is about 60% when it is heated to 1000 K. The initial cracking temperature of ammonia is 704 K, and the storage temperature of ammonia is 239 K. The total heat sink of ammonia when it is heated to 1000 K is calculated:

$$h_{\mathrm{fc}} = \Delta h\,|_{239}^{704} + 0.4 \cdot \Delta h\,|_{704}^{1000} + 0.6 \cdot 3180,$$

where Δh is the physical enthalpy difference of ammonia calculated by the National Institute of Standards and Technology (NIST). As shown in Fig. 3, when ammonia is heated to 1000 K in the microchannel, the total heat sink reaches 4800 kJ/kg.

In summary, ammonia has an outstanding cooling capacity and a higher equivalent calorific value than methane and kerosene. Besides, the combustion products of ammonia do not contain carbon, making it an environmentally friendly fuel.

3. System description

The configurations of the precooled cycle engines based on the PC-RT and PC-GT are shown in Figs. 5 and 6. As shown, according to the flight Mach numbers range, the operating modes of the precooled cycle engines can be divided into three modes, namely the turbine mode, the precooling mode, and the ramjet mode, which correspond to Mach 0-2.5, Mach 2.5-5, and above Mach 5, respectively. Their corresponding ideal pressure-volume (p-v) diagrams are shown in Figs. 7 and 8.

For the PC-RT, the engine is in the turbine mode when the flight Mach numbers are 0-2.5 (Fig. 5(a)). After being compressed by the intake and the compressor, the incoming air burns with the expanded fuel from the turbine exit in the combustor. The generated high-temperature gas is discharged through the nozzle to provide thrust for the vehicle. After being compressed by the fuel pump, the low-temperature fuel absorbs heat through the regenerative cooling heat exchanger on the wall of the combustor. The vaporized fuel expands and drives the turbine to compensate for the work consumed by the fuel pump and the compressor. The purposes of using the regenerative cooling heat exchanger are to vaporize the fuel so that it can fully expand to drive the turbine to do work and cool the combustor walls to ensure that they are below the temperature tolerance limit of the wall material. For the PC-GT, the engine is also in the turbine mode when the flight Mach numbers are 0-2.5 (Fig. 6(a)). After being compressed by the intake and the com-

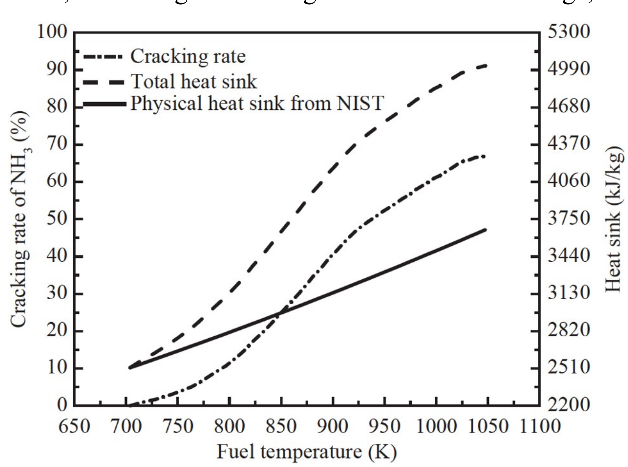

Figure 3 Calculated results of the ammonia heat sink.

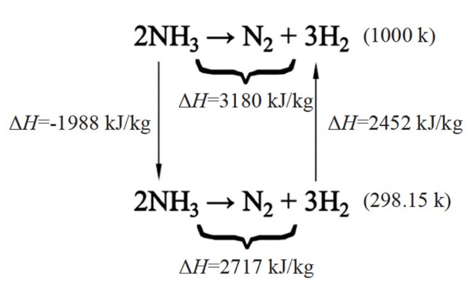

Figure 4 Schematic of the calculation of the heat of reaction at 1000 K.

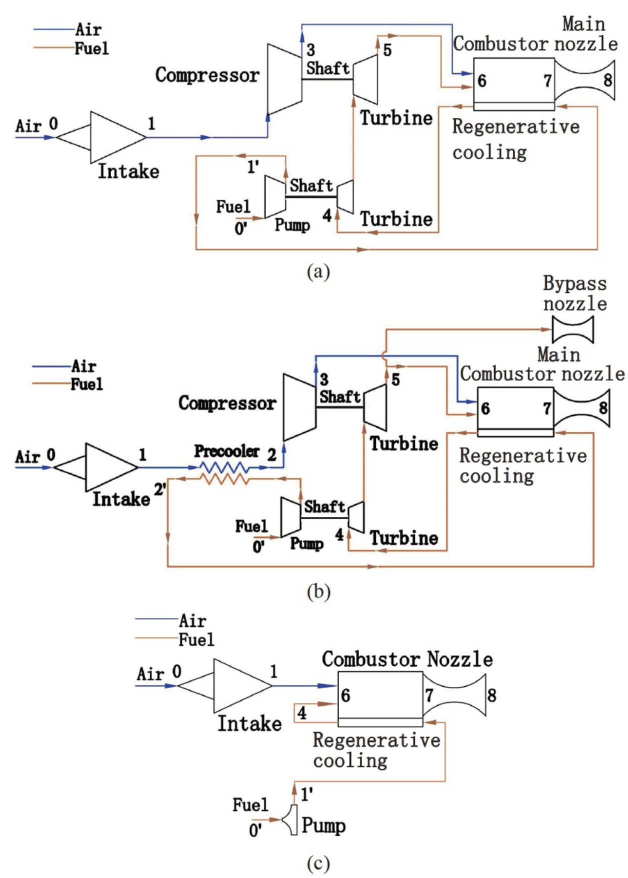

Figure 5 Schematic of the precooled cycle engine based on the PC-RT. (a) The turbine mode (Mach 0-2.5), (b) the precooling mode (Mach 2.5-5), (c) the ramjet mode (Mach > 5).

pressor, the incoming air enters the gas generator to burn with the fuel pumped by the fuel pump, which generates oxygen-rich gas to drive the turbine to do work. Here, it is assumed that the equivalence ratio of the fuel in the gas generator is 0.3. Then, the expanded oxygen-rich gas from the turbine enters the combustor to burn with the other part of the fuel pumped by the fuel pump, and the generated high-temperature gas is discharged through the nozzle to provide thrust for the vehicle. Similarly, the regenerative cooling heat exchanger is arranged on the combustor.

For the PC-RT, the engine turns into the precooling mode when the flight Mach numbers are 2.5-5 (Fig. 5(b)). The air compressed by the intake first passes through the precooler and is cooled by the low-temperature fuel. Then, it is further compressed by the compressor. Then, it burns with the expanded fuel from the turbine in the combustor. The generated high-temperature gas is discharged through the nozzle to provide thrust for the vehicle. After absorbing heat through the precooler and regenerative cooling heat exchanger, the fuel expands and drives the turbine to do work. When the flight Mach numbers are 2.5-5, to maintain a high thrust, the compressor needs to keep a high pressure ratio. So the cooling temperature of the air in the precooler outlet cannot be too high. For most fuels, they cannot cool the high-temperature air to a low temperature when the equivalence ratio is 1.0, so their amounts have to be increased. The combustion

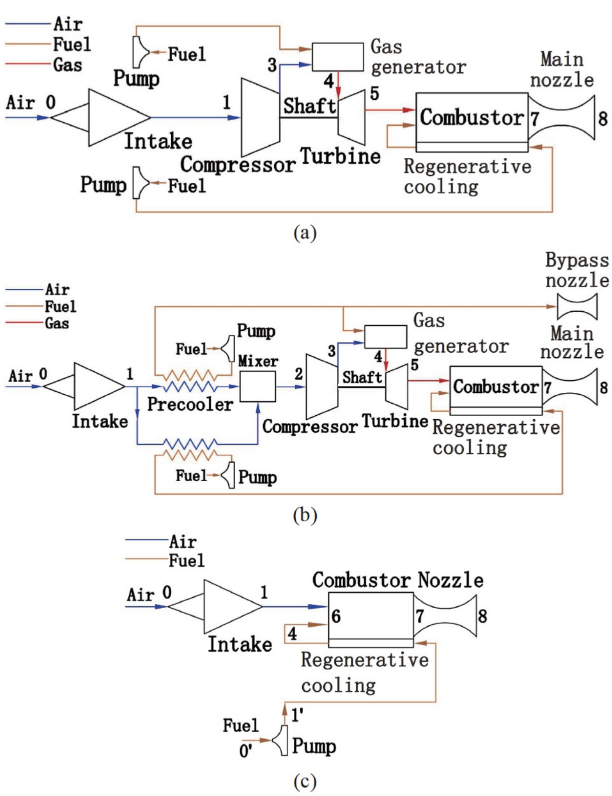

Figure 6 Schematic of the precooled cycle engine based on the PC-GT. (a) The turbine mode (Mach 0-2.5), (b) the precooling mode (Mach 2.5-5), (c) the ramjet mode (Mach > 5).

is arranged at the equivalence ratio of 1.0, and the rest fuel is discharged directly through the bypass nozzle to provide supplementary thrust for the vehicle. For the PC-GT, the engine is in the precooling mode when the flight Mach numbers are 2.5-5 (Fig. 6(b)). Compared with the turbine mode, the precooler is arranged before the compressor. Other working principles are similar to those in the turbine mode.

When the flight Mach numbers exceed 5, operated like a ramjet (Figs. 5(c) and 6(c)), after being compressed by the intake, the air directly enters the combustor and burns with the fuel. The generated high-temperature gas is discharged through the nozzle to generate thrust.

In Figs. 7 and 8, f is the actual fuel-air mass flow ratio. And f_{st} is the fuel-air mass flow ratio at the equivalence ratio of 1.0.

4. Modeling method

4.1 Turbine and precooling modes

4.1.1 Intake, compressor, turbine, combustor, and nozzle models

Equations based on the zero-dimensional thermodynamic

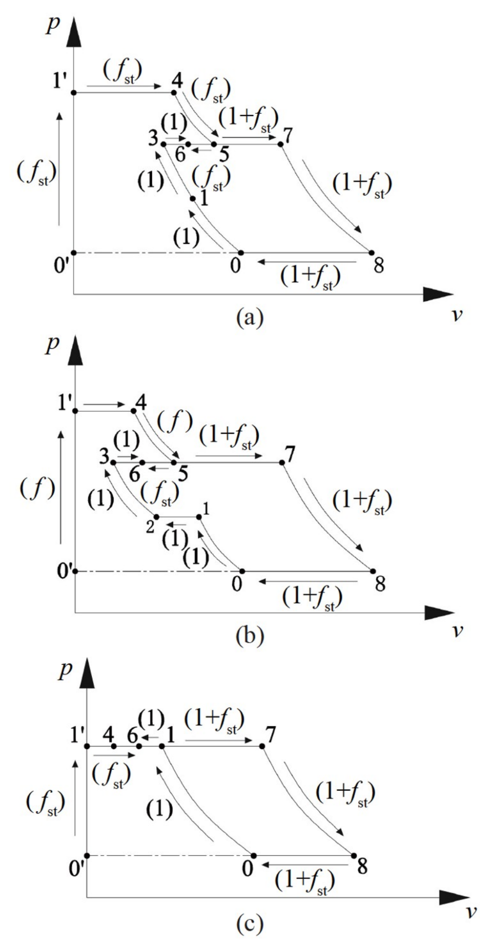

Figure 7 *p-v* diagram of the precooled cycle engine based on the PC-RT. (a) The turbine mode, (b) the precooling mode, (c) the ramjet mode.

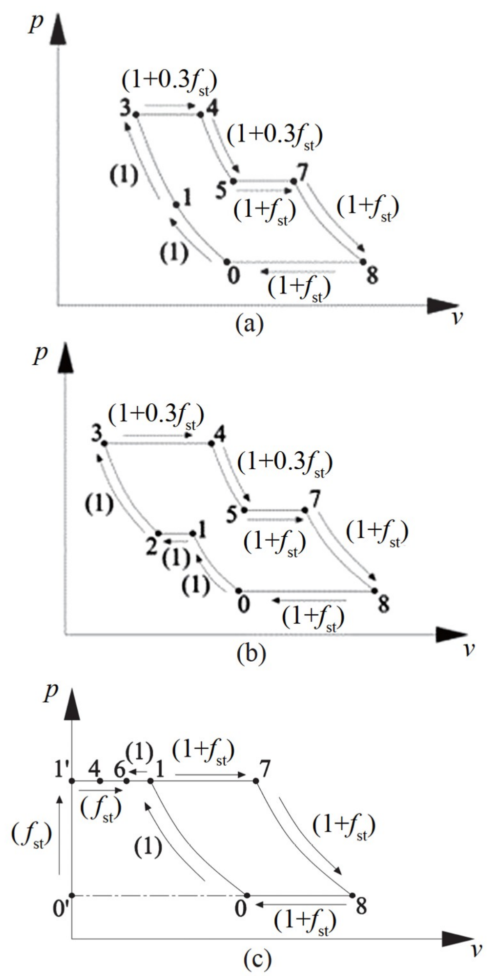

Figure 8 *p-v* diagram of the precooled cycle engine based on the PC-GT. (a) The turbine mode, (b) the precooling mode, (c) the ramjet mode.

models of the intake, the compressor, the turbine, the combustor, and the nozzle are listed in Table 1. Some engine operation parameters are listed in Table 2. For the intake, the calculation of the total pressure recovery coefficient is based on Ref. [30]. For the combustor, the combustion products are determined based on the minimum Gibbs free energy principle. In the case of ammonia and air, the combustion products are nitrogen and water when the equivalence ratio is 1.0.

The heat recovered ratio from the combustor is used to evaluate the ratio of the heat absorbed by the fuel in the regenerative cooling heat exchanger to the heat released by the fuel combustion,

$$\beta = \frac{Q_r}{f_{st} \cdot h_{PR} \cdot \eta_b}, \tag{3}$$

where Q_r is the heat absorbed by the fuel in the regenerative cooling heat exchanger from the combustor corresponding to a unit mass of air; f_{st} is the fuel-air mass flow ratio at the equivalence ratio of 1.0, the combustion is arranged at the equivalence ratio of 1.0; h_{PR} is the net calorific value of the fuel; η_b is the combustion efficiency.

4.1.2 Precooler model

The fluid-structure coupling heat transfer program is used to evaluate the cooling effects of fuels under different conditions. Figure 9 shows the precooler model used in this study and the mesh division in the heat transfer calculation domain. The model is also described in Ref. [31]. As shown, the high-temperature air and the fuel exchange heat are in the reverse directions. The fuel channel is a circular channel with an inner diameter of 1 mm, and the air channel is a triangular channel enclosed by the circular channels and fins. The precooler can be viewed as a whole consisting of multiple heat exchange units, with one heat exchange unit being the area enclosed by a single red regular hexagon in Fig. 9(b). The seven adjacent heat exchange units in Fig. 9(b) are taken as the heat transfer calculation domain, and the heat transfer of cold and hot fluids in the calculation domain can be equivalent to that of the whole precooler. In this study, the section area of the heat transfer calculation domain is assumed to be 216 mm^2, and the axial length of the heat transfer calculation domain is 700 mm. The mass flow rate of the high-temperature air is assumed to be 14 g/s in the heat transfer calculation domain.

As shown in Fig. 9, the program divides the heat transfer calculation domain of the precooler into many continuous cross sections along the axial direction, and the distance between the two adjacent cross sections is dx. The heat exchange between the two cross sections follows the energy and momentum equations:

$$\dot{m}_{i-1}\left(H_{i-1} + 1/2 \cdot u_{i-1}^2\right) = \dot{m}_i\left(H_i + 1/2 \cdot u_i^2\right) + \Delta H_i, \tag{4}$$

$$\dot{m}_{i-1}u_{i-1} + p_{i-1}A_{i-1} + \int_{i-1}^{i} p\mathrm{d}A = \dot{m}_i u_i + p_i A_i + \int_{i-1}^{i} \tau_w \mathrm{d}A. \tag{5}$$

ΔH_i is the difference in energy of the fluids between the two adjacent cross sections. The calculation equation is

$$\Delta H_i = q_i \cdot S_i \cdot \mathrm{d}x. \tag{6}$$

q_i is the heat flux of the fluids. The calculation equation is

$$q_i = h_i \cdot \left(T_i - T_{w,i}\right), \tag{7}$$

$$h_i = \frac{Nu_i \cdot \lambda_i}{D_h}. \tag{8}$$

Nu_i is the Nusselt number. The calculation equation is [32]

$$Nu = \frac{\frac{f}{2}\left(Re - 1000\right)Pr}{1 + 12.7\left(Pr^{2/3} - 1\right)\sqrt{\frac{f}{2}}}, \tag{9}$$

$$f = \frac{1}{4}\left(\frac{1}{1.8\lg Re - 1.5}\right)^2. \tag{10}$$

τ_w is the wall shear stress. The calculation equation is

$$\tau_w = f/2 \cdot \rho u^2. \tag{11}$$

The Fenics finite element calculation platform [33] is used

Table 1 Equations for the mathematical models in the turbine and precooling modes

Components	Calculation equation	No.
Intake	$P_{out} = P_{in} \cdot \left\{1 + [(\gamma - 1)/2]Ma^2\right\}^{\gamma/(\gamma-1)} \cdot \eta_{inta}$	(14)
	$T_{out} = T_{in} \cdot \left\{1 + [(\gamma - 1)/2]Ma^2\right\}$	(15)
	$\eta_{inta} = 0.95,\ (Ma \le 1.0)$ $\eta_{inta} = 0.95 \cdot \left[1 - 0.075(Ma - 1)^{1.35}\right],\ (1.0 < Ma \le 5.0)$ $\eta_{inta} = 0.95 \cdot \left[800/\left(Ma^4 + 935\right)\right],\ (5.0 < Ma)$	(16)
Compressor	$P_{out} = P_{in} \cdot \pi_{comp}$	(17)
	$T_{out} = T_{in} \cdot \left\{1 + \left(1/\eta_{comp}\right)\left[(\pi_{comp})^{(\gamma-1)/\gamma} - 1\right]\right\}$	(18)
	$w_{comp} = h_{comp,out} - h_{comp,in}$	(19)
Turbine	$P_{out} = P_{in}/\pi_{turb}$	(20)
	$T_{out} = T_{in} \cdot \left\{1 - \eta_{turb}\left[1 - \left(1/\pi_{turb}\right)^{(\gamma-1)/\gamma}\right]\right\}$	(21)
	$w_{turb} = h_{turb,in} - h_{turb,out}$	(22)
Combustor	$P_{out} = P_{in}$	(23)
	$\left(1 + f_{st}\right) \cdot c_{p\_g} \cdot T_{out} - \left(1 + f_{st}\right) \cdot c_{p\_g} \cdot T_{in} = f_{st} \cdot h_{PR} \cdot \eta_b \cdot (1 - \beta)$	(24)
	$\beta = Q_r/\left(f_{st} \cdot h_{PR} \cdot \eta_b\right)$	(25)
Nozzle	$u_{out} = \sqrt{2 \cdot c_{p\_g} \cdot T_{in} \cdot \left[1 - \left(p_{out}/p_{in}\right)^{(\gamma-1)/\gamma}\right]} \cdot \varphi$	(26)

Table 2 Engine operation parameters

Components	Symbol	Value
Fuel pump adiabatic efficiency	η_p	0.70
Compressor adiabatic efficiency	η_{comp}	0.80
Turbine adiabatic efficiency	η_{turb}	0.80
Combustion efficiency	η_b	0.90
Nozzle velocity coefficient	φ	0.98

to solve the partial differential equation for heat conduction to calculate the wall temperature of the heat transfer calculation domain. The wall material of the precooler is 1Cr18Ni9Ti, and its thermal conductivity is treated as a linear function of the wall temperature,

$$k = 0.01525T + 10.6. \quad (12)$$

The effectiveness of the precooler is used to evaluate the differences in the cooling effects of different fuels in the precooler [34],

$$\varepsilon = \frac{|T_{in} - T_{out}|_{max}}{(T_{h,in} - T_{c,in})}, \quad (13)$$

where $T_{h,in}$ and $T_{c,in}$ are the inlet temperatures of the air and fuel in the precooler, respectively. The numerator is the larger of the actual temperature difference between the inlet and outlet of the air or fuel.

4.2 Ramjet mode

Equations of the intake, the combustor, and the nozzle are listed in Table 3. Some engine operation parameters are listed in Table 4.

4.3 Performance parameters

Some performance parameters are adopted to measure the engine performance. They are listed in Table 5.

5. Validation of the model

5.1 Validation of the precooler model

Due to the lack of reported supercritical heat transfer experimental data for precoolers, in this study, we choose the experimental data on single-tube heating from Ref. [35] to validate the results of the heat transfer calculations. The comparison results are shown in Fig. 10. As shown, the calculated results agree well with the experiment results, with errors within 5%.

5.2 Validation of the thermodynamic cycle model

The ground test data of the ATREX engine with hydrogen as the fuel and coolant in Ref. [36] is quoted to verify the thermodynamic cycle model in this study. The comparison results are shown in Table 6. The calculated results agree well with the ground test data. Most errors are within 5%. It proves that the thermal cycle calculation method is feasible.

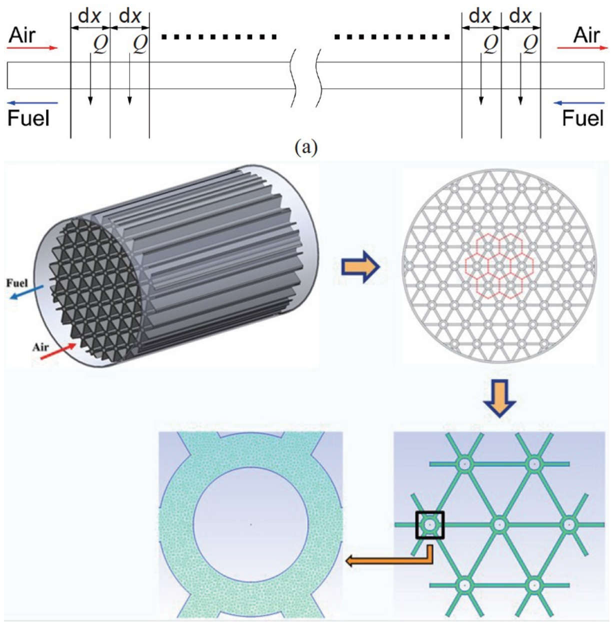

Figure 9 Schematic of the mesh division of the heat transfer calculation domain. (a) Axial mesh division, (b) cross-sectional mesh division.

6. Results and discussion

6.1 Cooling effects of different fuels

The cooling effects of four fuels, ammonia, hydrogen, methane, and kerosene in the precooler design in Sect. 4.1.2 are evaluated using the fluid-structure coupling heat transfer program. In the calculation, the air outlet temperature is set to the same value to compare the performance of the different fuels. The fuel inlet temperatures are their boiling point temperatures at atmospheric pressure, which are 239, 112, and 20 K for ammonia, methane, and hydrogen, respectively. For kerosene, this is 293 K. The cracking mechanism of kerosene can be referred to Ref. [31]. The fuel inlet pressure is 12 MPa. The length of the precooler is 700 mm. At Mach 3, the air inlet temperature is 601 K, and the air inlet pressure is 0.202 MPa. According to the calculation, the air outlet temperature is about 363 K, and the air outlet pressure is about 0.19 MPa. At Mach 4, the air inlet temperature is 890 K, and the air inlet pressure is 0.40 MPa. The air outlet temperature is about 482 K, and the air outlet pressure is about 0.39 MPa. At Mach 5, the air inlet temperature is 1247 K, and the air inlet pressure is 0.73 MPa. The air outlet temperature is about 527 K, and the air outlet pressure is about 0.723 MPa. The calculated outlet temperatures, effectiveness, and equivalence ratios of the fuels are listed in Table 7. As shown, the equivalence ratio requirement for ammonia is the lowest when the cooled air temperatures are nearly the same. The equivalent heat sink of ammonia can meet the cooling requirement of at least Mach 4, which means a lot to designers, because there is no further problem dealing with excess fuel other than that required for combustion.

The change in fluid temperature along the flow direction using ammonia as the coolant at the equivalence ratio of 1.0 is shown in Fig. 11. Due to the reverse flow of ammonia and air for heat exchange, the temperature of both is highest at the precooler inlet. There is a gentle slope in the ammonia temperature curve corresponding to the critical temperature. At Mach 3 and Mach 4 flight conditions, the ammonia outlet temperature is 438.6 and 775.3 K, respectively. The cracking rate is 0 and 7.3%, respectively, according to the curve in Fig. 2. Thus, for Mach 3-4 flight conditions, ammonia does not have a high cracking rate in the precooler without special treatment.

Table 3 Equations for the mathematical models in the ramjet mode

Components	Calculation equation	No.
Intake	$\psi = T_{\mathrm{out}}/T_{\mathrm{in}}$	(27)
	$P_{\mathrm{out}} = P_{\mathrm{in}} \cdot \left\{\psi/\left[\psi\left(1-\eta_c\right)+\eta_c\right]\right\}^{\gamma/(\gamma-1)}$	(28)
	$\eta_c = \left[\psi - \left(1/\eta_{\mathrm{inta}}\right)^{(\gamma-1)/\gamma}\right]/(\psi-1)$	(29)
Combustor	$P_{\mathrm{out}} = P_{\mathrm{in}}$	(30)
	$u_{\mathrm{out}} = u_{\mathrm{in}} \cdot \left\{\left(1+f_{\mathrm{st}} \cdot u_{\mathrm{fx}}/u_{\mathrm{in}}\right)/\left(1+f_{\mathrm{st}}\right) - \left(C_{\mathrm{f}} \cdot A_{\mathrm{w}}/A_{\mathrm{in}}\right)/\left[2\left(1+f_{\mathrm{st}}\right)\right]\right\}$	(31)

Table 4 Engine operation parameters

Components	Symbol	Value
Intake static temperature ratio	ψ	5
Combustor inlet velocity ratio of fuel to air	$u_{\mathrm{fx}}/u_{\mathrm{in}}$	0.5
Combustor resistance coefficient	$C_{\mathrm{f}} \cdot A_{\mathrm{w}}/A_{\mathrm{in}}$	0.2

6.2 Performance of the PC-RT in the turbine and precooling modes at Mach 2.5

This section compares the performance of the PC-RT in the turbine and precooling modes at Mach 2.5, which is a mode

Table 5 Equations for the performance of the engine

Components	Calculation equation	No.
Specific thrust (N/(kg/s))	$F_{\mathrm{SP}} = \left(1+f_{\mathrm{st}}\right) \cdot u_{\mathrm{MN}} + \left(f - f_{\mathrm{st}}\right) \cdot u_{\mathrm{BN}} - u_0$	(32)
Specific impulse (s)	$I_{\mathrm{SP}} = F_{\mathrm{SP}}/(f \cdot g)$	(33)
Overall efficiency (%)	$\eta_0 = F_{\mathrm{SP}} \cdot u_0/\left(f_{\mathrm{st}} \cdot h_{\mathrm{PR}} \cdot \eta_{\mathrm{b}}\right)$	(34)

transition Mach number, using ammonia as the fuel and coolant. Air precooling can effectively reduce the minimum β required to drive the turbine corresponding to the pumping pressure limit. The specific thrust at the equivalence ratio of 1.0 in the turbine and precooling modes is higher than that at the equivalence ratio of 0.8 in the precooling mode, and it turns out just the opposite for the specific impulse and overall efficiency.

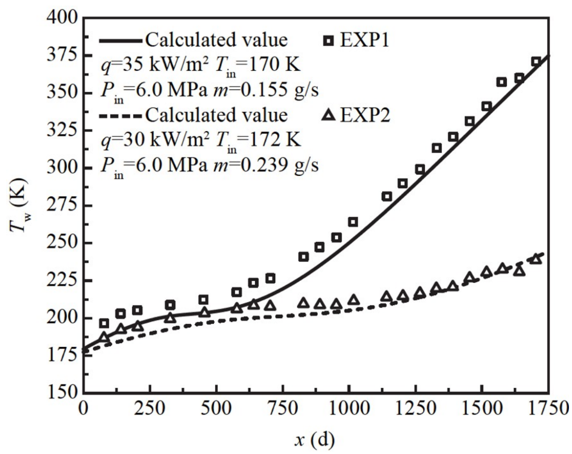

Figure 10 Comparison of the calculated inner wall temperature and the experimental values [35].

The physical properties of the ammonia cracking mixture are calculated using reference fluid thermodynamic and transport properties database (REFPROP), developed by NIST [37]. The flight dynamic pressure is 45 kPa for different Mach numbers. The pressure ratio of the compressor is 2.2. As shown in Fig. 12(c), the cracking rate curve of ammonia in Fig. 2 is partially extended to 1300 K according to its trend. The total temperature of the incoming air at Mach 2.5 is 486 K. The total pressure is 0.145 MPa. Based on the fluid-structure coupling heat transfer program, the air at 486 K can be cooled to 347 and 335 K when the equivalence ratio of ammonia is 0.8 and 1.0, respectively. If the pumping pressure of 20 MPa is set as the upper limit, the minimum required β corresponding to the limit is 10% and 8% for the precooling mode at the equivalence ratio of 0.8 and 1.0, respectively. And it is 18% for the turbine mode at the equivalence ratio of 1.0. It means that air precooling can effectively reduce the minimum heat required to drive the turbine absorbed from the combustor, which makes the heat exchanger design easier. If the minimum required β is to be reduced, the structure of the precooler needs to be optimized so that the air is cooled to a lower temperature while the fuel

Table 6 Comparison with the experimental results of Ref. [36]

Parameter	Ref. [36]	Calculation results (error)
Total temperature of incoming air (K)	287	287 (0)
Equivalence ratio	1.21	1.21 (0)
Air temperature at precooler exit (K)	172	172 (0)
Coolant initial temperature (K)	34.1	34.1 (0)
Coolant temperature at precooler exit (K)	243	266.58 (9.6%)
Air pressure at compressor entrance (kPa)	101	101 (0)
Compression ratio	3.7	3.7 (0)
Air pressure at compressor exit (kPa)	381	373.7 (1.9%)
Air temperature at compressor exit (K)	270	270 (0)
Coolant temperature at turbine entrance (K)	1379	1379 (0)
Coolant pressure at turbine entrance (kPa)	2086	2086 (0)
Expansion ratio of turbine	5.67	5.67 (0)
Coolant temperature at turbine exit (K)	1191	1200 (0.80%)
Coolant pressure at turbine exit (kPa)	368	368 (0)
Temperature of combustor (K)	2473	2473 (0)
Pressure of combustor (kPa)	381	373.7 (1.9%)
Gas temperature at heat exchanger exit in combustor (K)	2046	2160 (5.6%)
Expansion ratio of nozzle	3.8	3.8 (0)
Gas velocity at nozzle exit (m/s)	1165	1199 (2.9%)

Table 7 Cooling effects of different fuels

Fuel	Mach 3				Mach 4				Mach 5			
	$T_{fuel,out}$ (K)	ε	ϕ	$T_{air,out}$ (K)	$T_{fuel,out}$ (K)	ε	ϕ	$T_{air,out}$ (K)	$T_{fuel,out}$ (K)	ε	ϕ	$T_{air,out}$ (K)
NH_3	438.6	0.66	1.00	362.4	775.3	0.82	1.00	482.2(445*)	947.6(821*)	0.71	1.50	526.9
H_2	567.3	0.94	1.08	362.8	803.4	0.90	1.34	482.4	995.6	0.80	1.97	526.3
CH_4	551.7	0.90	2.77	362.6	765.4	0.84	3.30	482.3	923.9	0.72	4.70	527.0
Kerosene	442.0	0.77	10.0	363.3	667.0	0.68	6.20	482.6	776.0	0.75	8.50	526.8

* represents the result of calculations taking into account ammonia cracking.

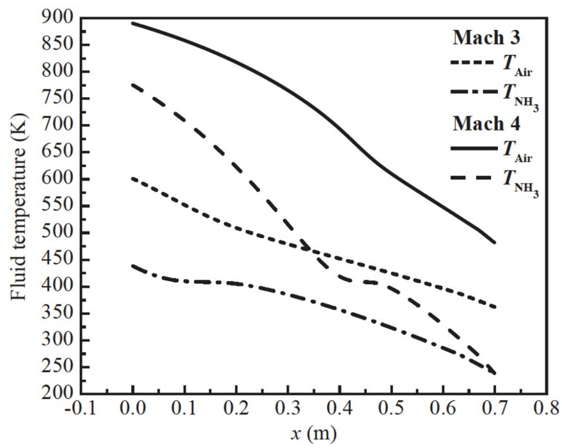

Figure 11 Change in fluid temperature along the flow direction using ammonia as the coolant.

is heated to a higher temperature in the precooler. In addition, the smaller the minimum required β, the larger the combustor size can be manufactured.

There is a total pressure drop of about 10% for the air in the precooler when the equivalence ratio is 1.0. Therefore, the specific thrust is lower than that in the turbine mode when β is less than 22%. As the fuel temperature at the turbine inlet increases, on the one hand, the increase in the fuel temperature at the combustor inlet and the increase in the hydrogen flow rate improve the specific thrust and specific impulse. On the other hand, the increase in the cracking rate means that the fuel must absorb more heat from the combustor, resulting in a decrease in the specific thrust and specific impulse. As shown in Fig. 12(c), the slope of the ammonia cracking rate curve decreases rapidly when the fuel temperature is greater than 1020 K. The increase in the specific thrust and specific impulse caused by the increase in the fuel temperature at the combustor inlet and the hydrogen flow rate is greater than the decrease in the specific thrust and specific impulse caused by the increase in heat absorption from the combustor. Therefore, the specific thrust and specific impulse begin to increase when the fuel temperature is greater than 1020 K. Accordingly, the overall efficiency begins to increase.

Due to the restriction of the minimum required β, the pressure ratio of the compressor in the turbine mode cannot take a high value. Taking the pressure ratio of 1.5 as an example, the minimum required β corresponding to the pumping pressure limit of 20 MPa can be reduced from 18% to 10.3% when the pressure ratio is reduced from 2.2 to 1.5 in the turbine mode at the equivalence ratio of 1.0. However, compared with the pressure ratio of 2.2 in the precooling mode (the minimum required β is 8%), the specific thrust decreases by about 5.0%. Thus, air precooling can increase the specific thrust within a reasonable range of β. An appropriate reduction in the equivalence ratio will increase the specific impulse but decrease the specific thrust. For example, in the precooling mode, the equivalence ratio of 0.8 increases the specific impulse by 6.2% but reduces the specific thrust by 15% compared with the equivalence ratio of 1.0.

In summary, air precooling can effectively reduce the minimum required β and thus reduce the design difficulty of the regenerative cooling heat exchanger. Air precooling can improve the engine performance within a reasonable range of β. The equivalence ratio of 1.0 is preferred if we want to increase thrust and solve the thrust gap problem at Mach 2.5. The equivalence ratio of 0.8 is preferred if we want to extend the cruising time of the vehicle and save fuel.

6.3 Performance of the PC-RT in the precooling mode at Mach 4

This section compares the performance of the PC-RT in the precooling mode at Mach 4 using ammonia, methane, and hydrogen as fuel and coolant. When the air outlet temperature in the precooler is nearly the same for the three fuels, ammonia has the highest specific thrust among the three fuels, and its specific impulse is higher than that of methane.

According to Table 7, when the equivalence ratios of ammonia, methane, and hydrogen are 1.0, 3.3, and 1.34, respectively, the effectiveness of the precooler can reach 0.82, 0.84, and 0.90, respectively. For ammonia, when the effectiveness is 0.82, based on Eq. (13), the ammonia outlet temperature in the precooler is 775.3 K, and the cracking rate is 7.3%. Based on the principle of energy conservation, the air outlet temperature in the precooler is about 445.0 K. The pressure ratio of the compressor is 2.2 for the three fuels. As shown in Fig. 13(d), W_P and W_{CP} are the work consumed by the fuel pump and the compressor, respectively. W_T is the work from the fuel vapor to drive the turbine. Compared with methane and hydrogen, when thermal cracking is considered, ammonia can cool the incoming air at 890 K to a lower temperature. Therefore, the work consumed by the compressor using ammonia is less than that using methane and hydrogen. When β is less than 12.7%, the fuel temperature at the turbine inlet of ammonia is the lowest among the three fuels, and its compatibility with the manufacturing materials of the regenerative cooling heat exchanger and turbine is the best. As shown in Fig. 13(e) and (f), ammonia has a higher specific thrust than methane and hydrogen, and a higher specific impulse than methane.

In summary, the highest fuel-air mass flow ratio at the equivalence ratio of 1.0 gives ammonia a higher specific thrust than methane and hydrogen. The highest fuel-air mass flow ratio at the equivalence ratio of 1.0 and thermal cracking give ammonia a higher equivalent heat sink than methane and hydrogen, which can meet the cooling requirement of at least Mach 4. To achieve nearly the same cooling effect in the precooler as ammonia, the fuel-air mass

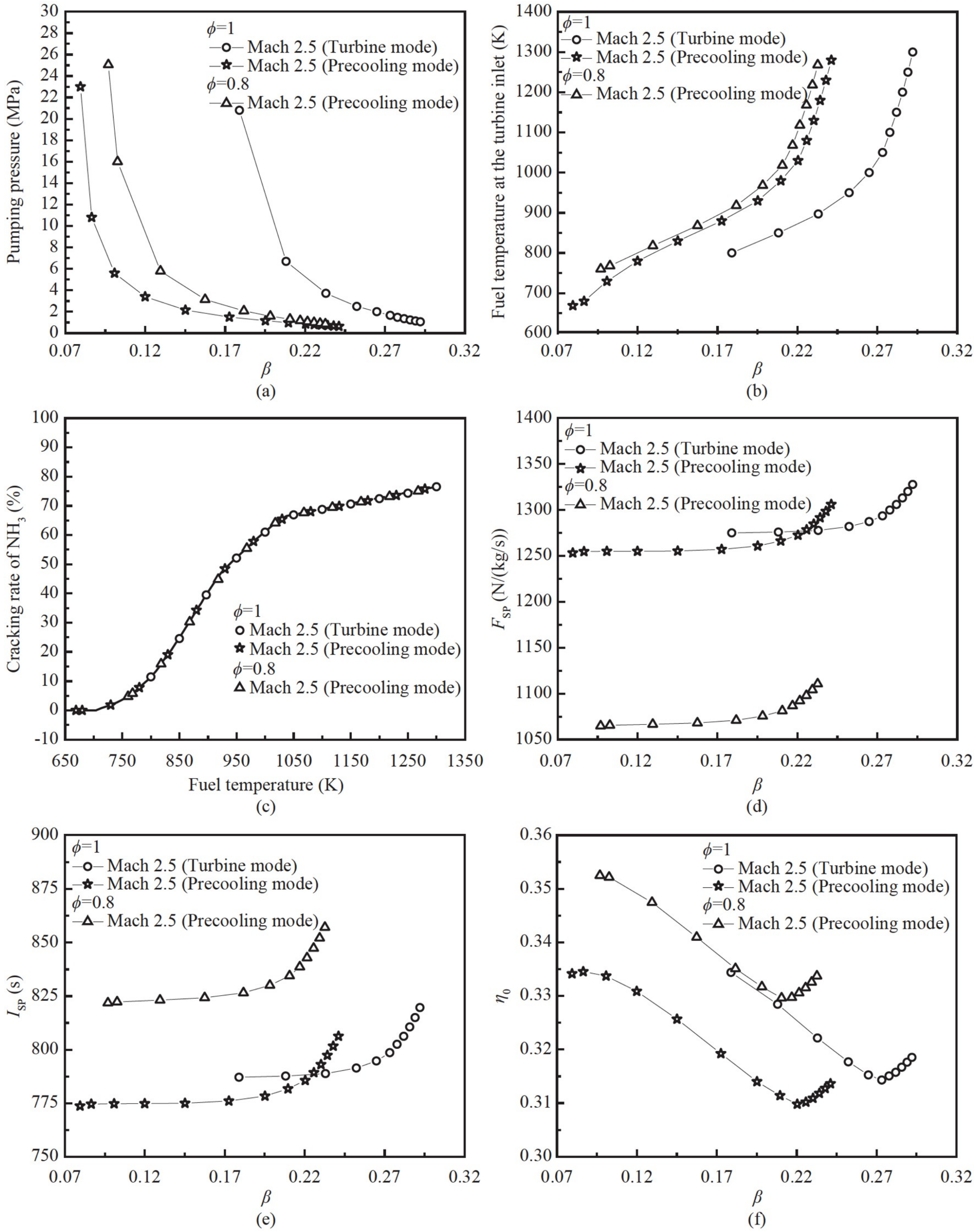

Figure 12 Comparison of performance of PC-RT in the turbine and precooling modes at Mach 2.5. (a) Pumping pressure, (b) fuel temperature at the turbine inlet, (c) cracking rate of NH_3, (d) specific thrust, (e) specific impulse, (f) overall efficiency.

flow ratio of methane and hydrogen must exceed that required for combustion. Therefore, the specific impulse of ammonia is higher than that of methane.

6.4 Performance of the PC-RT in the precooling mode at Mach 5

This section compares the performance of the PC-RT in the precooling mode at Mach 5 using ammonia, methane, and hydrogen as fuel and coolant. When the air outlet temperature in the precooler is nearly the same for the three fuels, the specific thrust of ammonia is higher than that of hydrogen, but slightly lower than that of methane when β is less than 12.8%. The specific impulse of ammonia is higher than that of methane.

According to Table 7, when the equivalence ratios of

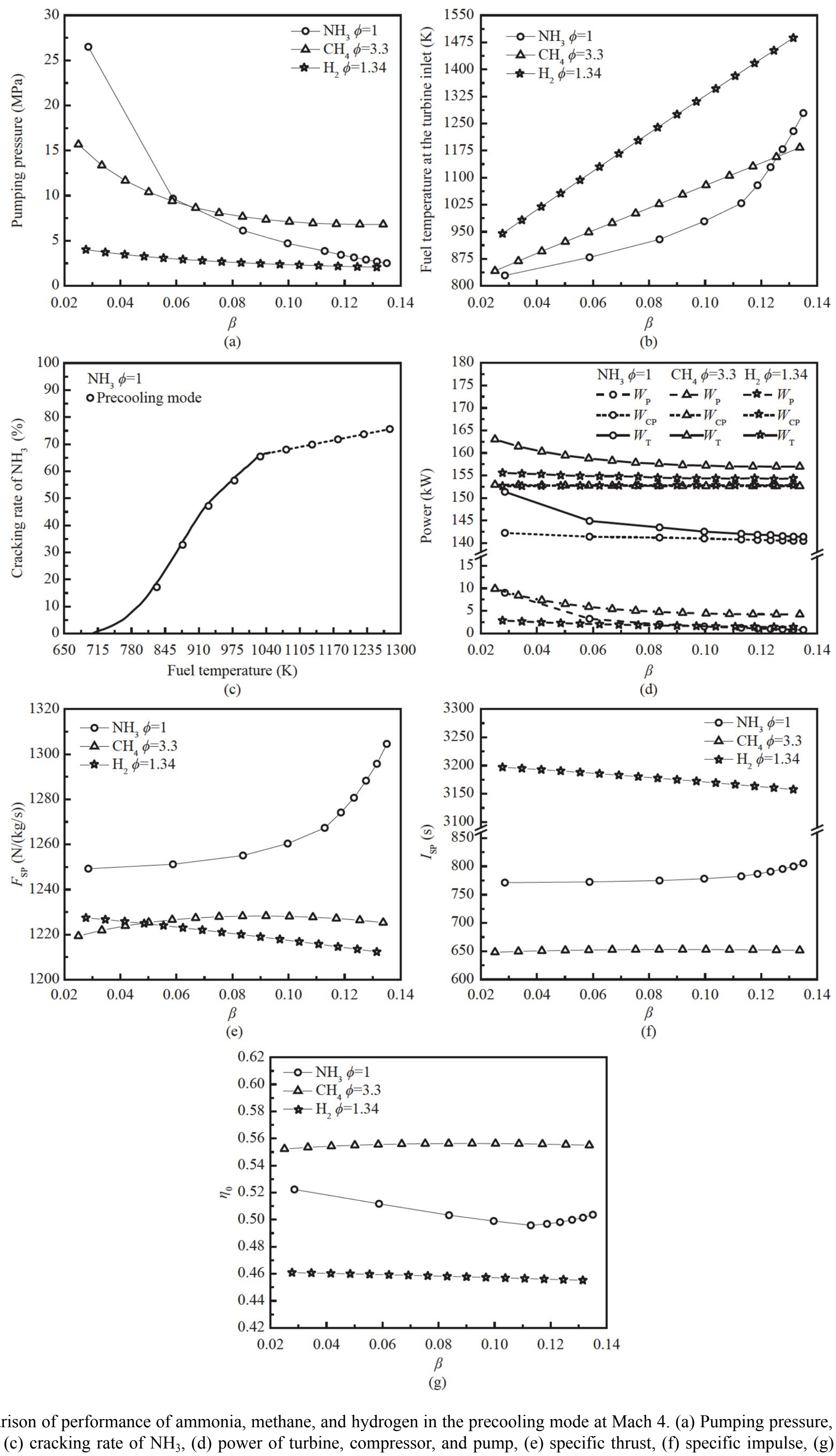

Figure 13 Comparison of performance of ammonia, methane, and hydrogen in the precooling mode at Mach 4. (a) Pumping pressure, (b) fuel temperature at the turbine inlet, (c) cracking rate of NH_3, (d) power of turbine, compressor, and pump, (e) specific thrust, (f) specific impulse, (g) overall efficiency.

ammonia, methane, and hydrogen are 1.5, 4.7, and 1.97, respectively, the effectiveness of the precooler can reach 0.71, 0.72, and 0.80, respectively. For ammonia, when the effectiveness is 0.71, based on Eq. (13), the air outlet temperature in the precooler is 526.9 K. Based on the principle of energy conservation, the ammonia outlet temperature in the precooler is about 821.0 K, and the cracking rate is 16.7%. As shown in Fig. 14(d), the work consumed by the compressor is nearly the same for the three fuels because the air outlet temperature in the precooler is nearly the same. The fuel temperature at the turbine inlet of ammonia is the lowest among the three fuels, and its compatibility with the manufacturing materials of the regenerative cooling heat exchanger and turbine is the best. As shown in Fig. 14(e) and (f), ammonia has a slightly lower specific thrust than methane when β is less than 12.8%, but a higher specific impulse than methane.

In summary, due to the increase in the equivalence ratio of methane, the supplementary thrust provided by methane discharged through the bypass nozzle increases. Therefore, the specific thrust of ammonia is slightly lower than that of methane when β is less than 12.8%. However, the specific impulse is higher for ammonia. The specific thrust of ammonia is higher than that of hydrogen.

6.5 Summary of performance of the PC-RT across a wide range of Mach numbers

This section compares the performance of the PC-RT at different Mach numbers using ammonia as the fuel and coolant. As the Mach number increases, the minimum β required to drive the turbine corresponding to the pumping pressure limit decreases. For the precooling mode at Mach 2.5-6, the PC-RT is easily implemented with the minimum required β less than 8%. Mach 4, where the minimum required β is 4%, is a sweet point because the specific impulse has not dropped significantly as it has at Mach 5 and 6. The equivalence ratio of 1.0 can meet the cooling requirement at Mach 4.

When the Mach number is 6, based on the heat transfer program, the effectiveness of ammonia is 0.79, with the incoming air at 1667 K cooled to about 543 K. According to the principle of energy conservation, the outlet temperature of ammonia in the precooler is about 848 K, and the cracking rate of ammonia is 24.3%. The pressure ratio of the compressor is 2.2. As shown in Fig. 15, as the Mach number increases, the minimum required β decreases. At Mach 5 and 6, ammonia does not need to absorb heat from the combustor and can meet the pumping pressure requirement by relying solely on the heat absorbed from the precooler. However, due to the increase in the equivalence ratio, the specific impulse has dropped significantly at Mach 5 and 6.

In summary, β is a key factor in the feasibility of the PC-RT. Within a reasonable range of β, the PC-RT using ammonia as the fuel and coolant can achieve high specific thrust. Its specific impulse is also much higher than that of the liquid oxygen/kerosene rocket engine (about 300 s). The feasibility of using ammonia in the PC-RT has been initially verified.

6.6 Summary of performance of the PC-RT and the PC-GT using different fuels at Mach 0-10

This section compares the performance of the precooled cycle engines based on the PC-RT and PC-GT over a wide speed range (Mach 0-10). Ammonia has the highest specific thrust among the four fuels. To effectively cool the incoming air, the fuel-air mass flow ratio of methane and kerosene must greatly exceed that required for combustion, resulting in a decrease in their specific impulse in the precooling mode. When using ammonia as the fuel and coolant, the performance of the PC-GT with a higher pressure ratio of the compressor is better than that of the PC-RT in the turbine mode, and the opposite is true in the precooling mode.

The specific thrust and specific impulse for different fuels are shown in Fig. 16. The equivalence ratio and air outlet temperature in the precooler for different fuels in the precooling mode are shown in Table 8. In the turbine mode, the equivalence ratio of hydrogen and methane remains at 1.0. When the pressure ratio of the compressor is 1.5, the pumping pressures of hydrogen and methane are less than 15 MPa for the Mach numbers of 1, 2, and 2.5 with the same β as ammonia.

Considering the low work capacity and coking of kerosene, the performance of the PC-RT using kerosene as the fuel and coolant is not calculated. As shown in Table 7, to achieve the same cooling effect as other fuels, the equivalence ratio of kerosene in the precooling mode must be very high, which is 10.0, 6.2, and 8.5 when the Mach numbers are 3, 4, and 5, respectively. Therefore, to reduce the kerosene energy waste, it is necessary to reduce the equivalence ratio appropriately. The pressure ratio and β are the same for the four fuels.

The specific thrust and specific impulse of the PC-RT corresponding to the pumping pressure of 15 MPa are shown in Fig. 16, using ammonia as the fuel and coolant in the turbine and precooling modes. For the turbine mode at Mach 2.5, when the pressure ratio of the compressor is 2.2, β corresponding to the pumping pressure of 15 MPa is 19.1%, which brings great difficulty to the design of the heat exchanger. Therefore, it is necessary to appropriately reduce the pressure ratio of the compressor in the turbine mode, which is set to 1.5, accordingly. In the turbine mode, when the pressure ratio of the compressor is 1.5, β corresponding to the pumping pressure of 15 MPa is 8.1%, 9.2%, and 10.9% when the Mach numbers are 1, 2, and 2.5, respec-

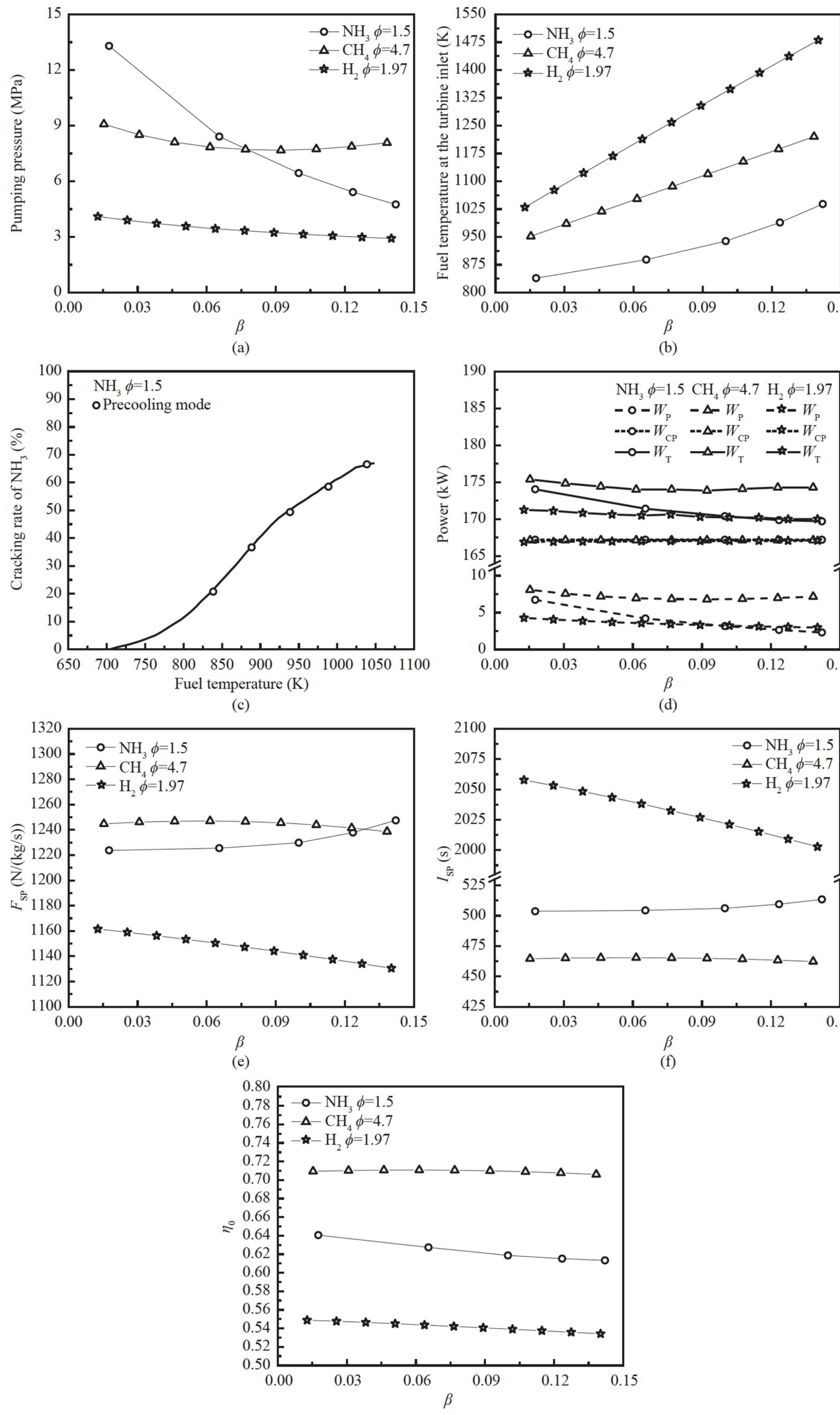

Figure 14 Comparison of performance of ammonia, methane, and hydrogen in the precooling mode at Mach 5. (a) Pumping pressure, (b) fuel temperature at the turbine inlet, (c) cracking rate of NH_3, (d) power of turbine, compressor, and pump, (e) specific thrust, (f) specific impulse, (g) overall efficiency.

tively. In the precooling mode, when the pressure ratio of the compressor is 2.2, β corresponding to the pumping pressure of 15 MPa is 8.4%, 7.5%, 4.9%, and 0.8% when the Mach numbers are 2.5, 3, 4, and 5, respectively. For the precooled cycle engine based on the PC-GT, the main factor limiting the increase in the pressure ratio of the compressor is not the minimum required β, but the air outlet temperature of the compressor. Therefore, in the turbine and precooling modes, the pressure ratio of the compressor of the PC-GT can take a higher value than that of the PC-RT. It is assumed that the pressure ratio of the compressor of the PC-GT is three times that of the PC-RT and that of the PC-GT is 4.5 and 6.6 for the turbine and precooling modes, respectively. And β of the PC-GT is consistent with that of the PC-RT at different Mach numbers in the turbine and precooling modes.

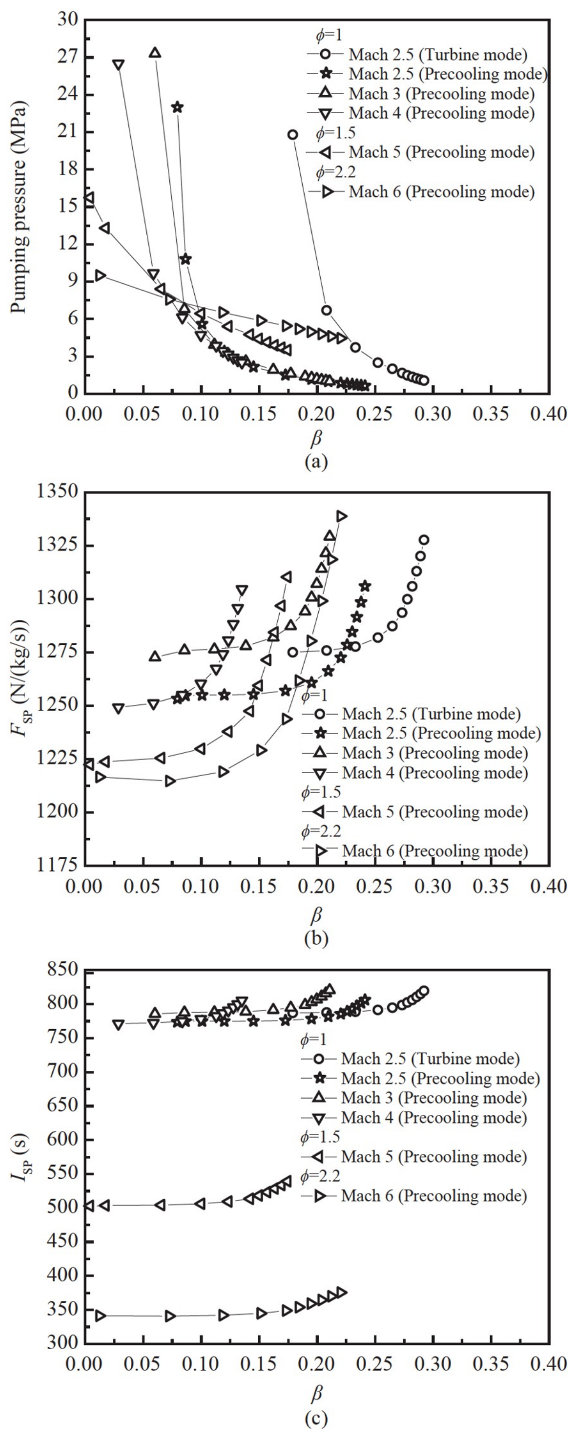

Figure 15 Summary of performance of ammonia at different Mach numbers. (a) Pumping pressure, (b) specific thrust, (c) specific impulse.

In the ramjet mode, the thermal cycle structure of the PC-RT is consistent with that of the PC-GT. Based on Sect. 4.2, the performance of the precooled cycle engines is also shown in Fig. 16, using ammonia, hydrogen, methane, and kerosene as fuel and coolant in the ramjet mode. The equivalence ratio of different fuels is 1.0. Limited by pyrolysis coking problems, the maximum Mach number using kerosene as the fuel and coolant generally does not exceed 8

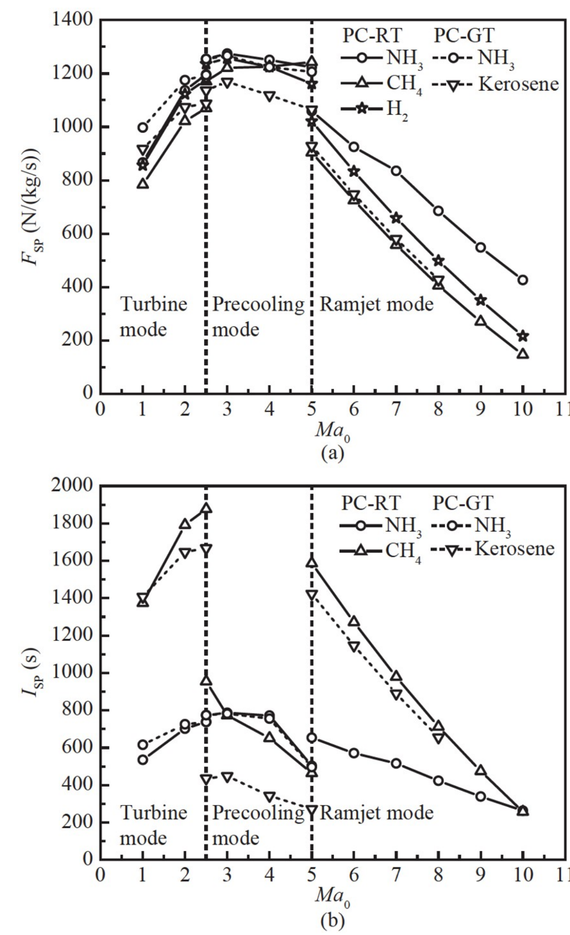

Figure 16 Summary of the engine performance at Ma 0-10. (a) Specific thrust, (b) specific impulse.

Table 8 The equivalence ratio and air outlet temperature in the precooler for different fuels

$\phi/T_{air,out}$ (K)	NH_3	CH_4	H_2	Kerosene
Mach 2.5	1.00/335.0	2.15/334.0	1.00/304.0	4.00/384.2
Mach 3	1.00/362.4	2.77/362.6	1.08/362.8	4.00/433.3
Mach 4	1.00/445.0	3.30/482.3	1.34/482.4	5.00/512.0
Mach 5	1.50/526.9	4.70/527.0	1.97/526.3	6.00/600.0

[38]. For ammonia, the heat flux on the combustor wall is assumed to be 1-5 MW/m^2 when the Mach numbers are 6-10. The inner diameter of a single regenerative cooling channel is assumed to be 1 mm, the length is 1.5 m, and the flow rate of ammonia in a single channel is 1.25 g/s. The cracking rate can be calculated from the above assumptions, as can the specific thrust and specific impulse.

As shown in Fig. 16, when using ammonia as the fuel and coolant, the specific thrust and specific impulse of the PC-GT with a pressure ratio of 4.5 are higher than those of the PC-RT with a pressure ratio of 1.5 in the turbine mode. The specific thrust and specific impulse of the PC-RT with a pressure ratio of 2.2 are higher than those of the PC-GT with a pressure ratio of 6.6 in the precooling mode. For the PC-RT in the turbine mode, the specific thrust of ammonia is similar to that of hydrogen and higher than that of methane. However, the specific impulse of ammonia is lower than that of hydrogen and methane. For the PC-RT in the precooling mode, the specific thrust of ammonia is higher than that of hydrogen and methane, and the specific impulse of ammonia is higher than that of methane at Mach 4 and 5. For the PC-GT in the turbine mode, when the equivalence ratio of ammonia and kerosene is 1.0, the specific thrust of ammonia is higher than that of kerosene. The specific impulse of ammonia is lower than that of kerosene. For the PC-GT in the precooling mode, as the equivalence ratio of kerosene increases, the specific impulse of kerosene decreases rapidly. The specific thrust and specific impulse of ammonia are higher than those of kerosene. In the ramjet mode, the specific thrust of ammonia is higher than that of other fuels. However, the specific impulse of ammonia is lower than that of other fuels.

In summary, for the PC-GT in the turbine mode, its performance is not limited by the pumping pressure, so its specific thrust and specific impulse with a pressure ratio of 4.5 are higher than those of the PC-RT with a pressure ratio of 1.5. For the PC-RT in the precooling mode, ammonia can absorb heat from the precooler and combustor to drive the turbine to do work, which alleviates the restriction of the pumping pressure on its performance, so its specific thrust and specific impulse with a pressure ratio of 2.2 are higher than those of the PC-GT with a pressure ratio of 6.6. Therefore, in the turbine mode, the PC-GT is preferred. In the precooling mode, the PC-RT is preferred because it can greatly reduce the pressure ratio of the compressor while maintaining good performance. Moreover, the PC-RT does not contain a gas generator in its structure. Therefore, the weight of the PC-RT can be lower than that of the PC-GT. Compared with other fuels, the advantages of ammonia in the precooling mode are highlighted due to its highest equivalent heat sink. In the turbine and ramjet modes, although its specific thrust is the highest among the four fuels, its specific impulse is lower than that of other fuels.

7. Conclusion

In this study, we analyze two thermal cycles with ammonia as the fuel and coolant, namely the PC-RT and PC-GT, which use the onboard fuel and the high-temperature oxygen-rich gas to drive the turbine to do work, respectively. By modeling and analyzing the two thermal cycles, their performances with ammonia, hydrogen, methane, and kerosene as fuel and coolant are compared, and the feasibility of using ammonia in the two thermal cycles is initially verified. The following conclusions can be drawn.

(1) The operating modes of the precooled cycle engines based on the PC-RT and PC-GT can be divided into three modes, namely the turbine mode, the precooling mode, and the ramjet mode, with speed ranges corresponding to Mach 0-2.5, Mach 2.5-5 and above Mach 5, respectively. The purpose of setting the precooling mode is to solve the bottleneck problems of the narrow operating range of the compressor and insufficient thrust at Mach 2.5-5.

(2) A fluid-structure coupling heat transfer program is developed to evaluate the cooling effects of different fuels on the incoming high-temperature air. The result shows that the equivalent heat sink of ammonia is higher than that of hydrogen, methane, and kerosene, and can meet the cooling requirement of at least Mach 4 in the precooling mode, providing sufficient flexibility for the design of various engines in a wide speed range.

(3) For the PC-RT at Mach 2.5, the performance in the precooling mode is compared with that in the turbine mode using ammonia as the fuel and coolant. The result shows that air precooling can alleviate the restriction of the pumping pressure on the minimum required β and increase the specific thrust within a reasonable range of β. The smaller the minimum required β is, the less difficult the heat exchanger design is. Reducing the equivalence ratio increases the specific impulse but decreases the specific thrust and increases the minimum required β.

(4) The performance of the precooled cycle engines based on the PC-RT and PC-GT is compared using ammonia, hydrogen, methane, and kerosene as fuel and coolant at Mach 0-10. The result shows that the PC-GT is preferred in the turbine mode, and the PC-RT is preferred in the precooling mode. The specific thrust of ammonia is greater than that of other fuels due to its highest fuel-air mass flow ratio at the equivalence ratio of 1.0, which indicates that ammonia has better acceleration performance than other fuels and is suitable for the first-stage power of the two-stage vehicle. The performance advantages of ammonia are the most evident in the precooling mode due to its highest equivalent heat sink.

(5) The application of ammonia has broadened the choice of fuel family for precooled cycle engines. The advantages of no carbon emission, low cost, high density, high specific

thrust, and high heat sink make it a potential alternative to hydrogen in the Mach 0-10 flight range.

Conflict of interest *On behalf of all authors, the corresponding author states that there is no conflict of interest.*

Author contributions ***Xin Zhang:*** *Conceptualization, Methodology, Software, Investigation, Formal Analysis, Writing – original draft.* ***Yang Lu:*** *Conceptualization, Funding Acquisition, Resources, Supervision, Writing – review & editing.* ***Xuejun Fan:*** *Conceptualization, Funding Acquisition, Resources, Supervision, Writing – review & editing.*

Acknowledgements *This work was supported by the High-level Innovative Research Institute from the Department of Science and Technology of Guangdong Province (Grant No. 2020B0909010003), and the Ministry of Education of China (Grant No. 8091B02052401).*

1 M. J. Bulman, and A. Siebenhaar, in Combined cycle propulsion: Aerojet innovations for practical hypersonic vehicles: Proceedings of the 17th AIAA International Space Planes and Hypersonic Systems and Technologies Conference, San Francisco, 2011.
2 Y. Wei, Major technological issues of aerospace vehicle with combined-cycle propulsion, Aerosp. Technol. **52**, 1 (2022).
3 Z. P. Zou, Y. F. Wang, Q. T. Eri, R. C. Zhang, R. Zhao, and M. Z. Chen, Research progress on hypersonic precooled airbreathing engine technology, Aeroengine **47**, 8 (2021).
4 D. M. Zhu, M. Chen, H. L. Tang, and J. Zhang, "Over-under" concept hypersonic turbo-ramjet combined propulsion system, J. Beijing Univ. Aeronaut. Astronaut. **32**, 263 (2006).
5 R. H. Zheng, and C. B. Chen, Overview of solution to TBCC engine thrust trap problem, J. Rocket Propuls. **47**, 21 (2021).
6 P. Carter, and V. Balepin, in Mass injection and pre-compressor cooling engines analyses: Proceedings of the 38th AIAA/ASME/SAE/ASEE Joint Propulsion Conference and Exhibit, Indianapolis, 2002.
7 Z. Wang, Y. Wang, J. Zhang, and B. Zhang, Overview of the key technologies of combined cycle engine precooling systems and the advanced applications of micro-channel heat transfer, Aerosp. Sci. Tech. **39**, 31 (2014).
8 A. Q. Lin, Q. Zheng, F. Wu, H. Yang, and H. Zhang, Investigation on mass injection precooling technology of aero-turbine engine, J. Propuls. Technol. **41**, 721 (2020).
9 C. Lv, H. Xu, F. Quan, J. Chang, and D. Yu, Thermodynamic modeling and analysis of ammonia injection pre-compressor cooling cycle: A novel scheme for high Mach number turbine engines, Energy Convers. Manage. **265**, 115776 (2022).
10 K. Harada, N. Tanatsugu, and T. Sato, Development study of a precooler for the air-turboramjet expander-cycle engine, J. Propuls. Power **17**, 1233 (2001).
11 N. Tanatsugu, T. Sato, V. Balepin, K. Harada, H. Kobayashi, Y. Naruo, H. Hatta, Y. Kogo, T. Kashiwagi, T. Mizutani, J. Omi, K. Hamabe, J. Tomike, R. Minami, and J. Kretschmer, in Development study on ATREX engine: Proceedings of the Space Plane and Hypersonic Systems and Technology Conference, Norfolk, 1996.
12 J. M. Luo, S. H. Yang, J. Q. Zhang, J. Li, Z. Z. Xiang, and W. Z. Zhang, Performance analysis of expander cycle air-turborocket with methane-precooled, J. Propuls. Technol. **42**, 1964 (2021).
13 H. Taguchi, H. Futamura, R. Yanagi, and M. Maita, in Analytical study of pre-cooled turbojet engine for TSTO spaceplane: Proceedings of the 10th International Space Planes and Hypersonic Systems and Technologies Conference, Kyoto, 2001.
14 H. Taguchi, H. Kobayashi, T. Kojima, A. Ueno, M. Hongoh, K. Harada, and T. Aoki, in Hypersonic flight experiment plan of pre-cooled turbojet engine: Proceedings of the 18th AIAA/3AF International Space Planes and Hypersonic Systems and Technologies Conference, Tours, 2012.
15 R. Varvill, and A. Bond, A comparison of propulsion concepts for SSTO reusable launchers, J. Br. Interplanet. Soc. **56**, 108 (2003).
16 R. Longstaff, and A. Bond, in The SKYLON project: Proceedings of the 17th AIAA International Space Planes and Hypersonic Systems and Technologies Conference, San Francisco, 2011, pp. 2011-2244.
17 H. Taguchi, H. Kobayashi, T. Kojima, M. Hongoh, D. Masaki, and S. Nishida, in Performance evaluation of hypersonic pe-cooled turbojet engine: Proceedings of the 20th AIAA International Space Planes and Hypersonic Systems and Technologies Conference, Glasgow, 2015.
18 Y. Yao, Z. X. Wang, X. B. Zhang, and L. Zhou, Modeling and cycle characteristics analysis of liquid hydrogen pre-cooled air-breathing engine, J. Propuls. Technol. **43**, 26 (2022).
19 X. Yu, W. Yu, C. Wang, and D. Yu, Thermodynamic analysis of the influential mechanism of fuel properties on the performance of an indirect precooled hypersonic airbreathing engine and vehicle, Energy Convers. Manage. **196**, 1138 (2019).
20 Y. Lu, and X. J. Fan, in Concept design of a high-speed precooled air-breathing engine using methane: Proceedings of the 13th National Conference on Hypersonic Technology, Xiamen, 2021.
21 C. Wang, C. Ha, X. Pan, J. Qin, and H. Huang, Thermodynamic analysis of chemical precooled turbine combined engine cycle, Energy Convers. Manage. **239**, 114184 (2021).
22 C. Wang, Y. Feng, Z. Liu, Y. Wang, J. Fang, J. Qin, J. Shao, and H. Huang, Assessment of thermodynamic performance and CO_2 emission reduction for a supersonic precooled turbine engine cycle fueled with a new green fuel of ammonia, Energy **261**, 125272 (2022).
23 C. Cai, Q. Zheng, J. Fang, H. Chen, C. Chen, and H. Zhang, Performance assessment for a novel supersonic turbine engine with variable geometry and fuel precooled: From feasibility, exergy, thermoeconomic perspectives, Appl. Therm. Eng. **225**, 120227 (2023).
24 E. P. Perman, G. A. S. Atkinson, and W. Ramsay, The decomposition of ammonia by heat., Proc. R. Soc. Lond. **74**, 110 (1905).
25 S. Chiuta, R. C. Everson, H. W. J. P. Neomagus, P. van der Gryp, and D. G. Bessarabov, Reactor technology options for distributed hydrogen generation via ammonia decomposition: A review, Int. J. Hydrogen Energy **38**, 14968 (2013).
26 S. R. Deshmukh, A. B. Mhadeshwar, and D. G. Vlachos, Microreactor modeling for hydrogen production from ammonia decomposition on ruthenium, Ind. Eng. Chem. Res. **43**, 2986 (2004).
27 S. Mukherjee, S. V. Devaguptapu, A. Sviripa, C. R. F. Lund, and G. Wu, Low-temperature ammonia decomposition catalysts for hydrogen generation, Appl. Catal. B-Environ. **226**, 162 (2018).
28 X. Zhang, Y. Lu, D. Cheng, and X. J. Fan, Analysis of performance of ammonia airbreathing variable cycle engine, Chin. J. Theor. Appl. Mech. **54**, 3223 (2022).
29 X. Yu, X. Pan, J. Zheng, C. Wang, and D. Yu, Thermodynamic spectrum of direct precooled airbreathing propulsion, Energy **135**, 777 (2017).
30 J. Q. Zhu, G. P. Huang, and Z. J. Lei, Aerothermo Dynamics of Aeroengine lntake and Exhaust System (Shanghai Jiao Tong University Press, Shanghai, 2014).
31 Z. X. Chen, Y. Lu, and X. J. Fan, A counter-flow fin-tube air precooler design and its flow heat exchange calculation method, J. Propul. Technol. **44**, 152 (2023).
32 H. Chang, J. Lian, T. Ma, L. Li, and Q. Wang, Design and optimization of an annular air-hydrogen precooler for advanced space launchers engines, Energy Convers. Manage. **241**, 114279 (2021).
33 K. Valen-Sendstad, and D. A. Steinman, in CFD challenge: Solutions using a finite element method flow solver implemented in FEniCS: Proceedings of the ASME 2012 Summer Bioengineering Conference, Fajardo, 2012.
34 S. M. Yang, and W. Q. Tao, Heat Transfer (Higher Education Press, Beijing, 2006).
35 H. Li, Z. L. Ru, Z. P. Zou, and S. Z. Zhou, Investigation on heat transfer characteristic of supercritical methane in a microtube, J. Nanjing Univ. Aeronaut. Astronaut. **53**, 513 (2021).

36 H. Kobayashi, N. Tanatsugu, and T. Sato, in Themal management of precooler ATREX engine with expander cycle: Proceedings of the 14th International Symposium on Air Breathing Engines, Florence, 1999.
37 Y. Higashi, NIST thermodynamic and transport properties of refrigerants and refrigerant mixtures (REFPROP), Netsu Bussei, **14**, 2 (2000).
38 P. Moses, in X-43C plans and status: Proceedings of the 12th AIAA International Space Planes and Hypersonic Systems and Technologies, Norfolk, 2003.

以氨为燃料和冷却剂的预冷循环发动机热力学性能评估

张鑫, 陆阳, 范学军

摘要 为了满足马赫数0-10宽域飞行器对吸气式动力的需求, 分析了两种以氨为燃料和冷却剂的热力循环, 即预冷火箭-涡轮循环和预冷燃气涡轮循环. 首先, 将预冷循环发动机的工作模态分为涡轮模态、预冷模态和冲压模态; 其次, 采用流固耦合换热程序, 评估了不同燃料对来流高温空气的冷却效果. 结果表明, 氨的当量热沉高于其他燃料, 在预冷模态下至少可以满足马赫4来流的冷却需求, 再次, 比较了马赫2.5时预冷火箭-涡轮循环在涡轮和预冷模态下的性能. 结果表明, 空气预冷减轻了泵压对最小需求β的限制, 在合理的β范围内提高了比推力; 最后, 比较了使用不同燃料时预冷循环发动机的性能. 结果表明, 氨的比推力大于其他燃料, 由于氨的当量热沉最高, 因此在预冷模态下氨的性能优势最为明显. 综上所述, 本文介绍的以氨为燃料和冷却剂的预冷循环发动机具有无碳排放、成本低、比推力大、冷却通道不会被裂解产物堵塞等优点. 它们适用于两级飞行器的第一级动力和高马赫数吸气式飞行等应用场景.